

Spectroscopy, electronic structure and quantification attempt in the spectral range of the Li K α emission band

Philippe Jonnard^{1*}

¹ Sorbonne Université, Faculté des Sciences et Ingénierie, Laboratoire de Chimie Physique - Matière et Rayonnement, UMR CNRS, 4 place Jussieu, 75005 Paris, France

Abstract. In this work, we present the way we perform high-resolution wavelength-dispersive X-ray spectrometry in the ultra-soft X-ray range. For this purpose, we use a reflection zone plate spectrometer working, as a variable line spacing grating spectrometer, in the 40 – 110 eV spectral range. We show that the shape of the emission bands can be reproduced by simulation of spectra obtained from the local and partial density of states calculated with the density functional theory. The knowledge of the electronic structure of the material under consideration is important to properly interpret the spectra, which can be complicated when many elements are present in the sample, such as the amblygonite phosphate. We also show the first attempt of elemental quantification of an AlCuLi alloy from intensities measured with the reflection zone plate spectrometer. The obtained mass fractions are in good agreement with those obtained in a standard way from measurements performed in the soft X-ray range with crystal spectrometers.

1 Introduction

Different ways to perform X-ray emission spectroscopy exist [1,2]: energy-dispersive X-ray spectrometry (EDS) and wavelength-dispersive X-ray spectrometry (WDS). However, the X ray spectral range is very wide: photon energies spread from a few tens of eV to hundreds of keV. Then, depending on the considered range, different spectrometers can be relevant, each with their own capabilities in terms of spectral resolution, collected intensities, acquisition speed, etc. However, in the range of the Li K α emission band around 50 eV (25 nm), *i.e.*, in the ultra-soft X-ray range, very few studies are published.

Regarding EDS, to our knowledge it is not possible to find in the literature studies performed with bolometers measuring the Li K α emission [3]. These devices measured the detected photon energy from the temperature rise in a sensitive thermometer. In the Li K range a spectral resolution of only a few eV is expected, which would be very interesting to avoid spectral interferences and to be sensitive to the chemical state of the lithium atoms. Silicon drift detectors can also be employed provided no window is set up at their entrance. Their advantage is their efficiency, particularly if many quadrants are used. However, they

* Corresponding author: philippe.jonnard@sorbonne-universite.fr

suffer from medium energy resolution, of a few tens of eV, and only a few studies are published as for example this one [4].

Regarding WDS, owing to the long wavelength of the ultra-soft X-ray radiation, it is not possible to find crystals having sufficiently large d-spacings (or reticular distances) to fulfil the Bragg law. Artificial crystals, in fact periodic multilayers, can be used. Their advantage is that they can be custom designed for the considered spectral range and generally lead to relatively high collected intensities but to medium spectral resolution. In the Li K range, a resolution of a few eV can be obtained [5,6]. However, in crystals spectrometers, such as Johann or Johansson configurations [7], widely used in electron probe microanalysers (EPMA) or scanning electron microscopes (SEM), windows are necessary leading to a large attenuation of the ultra-soft radiation. Provided special design of the windows, this kind of spectrometer can be useful [8]. Another mean to perform WDS is to use grating spectrometers: They rely on the grating law [7] and are well suited to work at high-spectral resolution in the ultra-soft X-ray range. Since the development of variable line spacing grating and their recent setup in electron microscopes and EPMA [9,10], it is possible to work in the Li K range without scanning the detection angles, that is to say to obtain spectra with fixed CCD cameras.

In this presentation, we describe the use of a reflection zone plate spectrometer, working in the 40 – 110 eV photon energy range on the same principle as the variable line spacing grating spectrometer. Owing that the emissions lying in the ultra-soft X-ray range are mainly emission bands, *i.e.*, emission coming from electron transition from the valence band to a core hole, they can be described from density of states (DOS) calculations and are sensitive to the chemical state of the emitting element. We show, on some examples regarding some oxide compounds that the emission bands can be divided in two parts and this can be helpful to interpret the spectra of some minerals. Finally, we present an attempt to perform elemental quantification on a quasi-crystal.

2 Reflection zone plate spectrometer

The reflection plate spectrometer (RZP) has been developed several years ago [11]. The dispersion of the polychromatic incident radiation coming from the sample relies on the grating law [7]. The present spectrometer (from Nanooptics-Berlin: <https://www.nanooptics-berlin.com>) is described in [12] and its scheme is shown in figure 1. The dispersion of the polychromatic X-ray beam coming from the sample is performed through a reflection zone plate. The RZP is working as a variable line spacing grating allowing to focus the different wavelengths on a flat field, so avoiding any scanning and thus limiting the acquisition time. The detection is done with a back-illuminated CCD camera from Greateyes (ALEX-s) operating at -60°C.

At the first diffraction order, the spectrometer works in the 40 – 110 eV spectral range. The energy calibration is performed with the high order diffracted peaks of the C K α emission of a graphite reference sample. The spectrometer is set up on a CAMECA SX100 EPMA. It is currently not possible to use simultaneously the bent-crystal and RZP spectrometers, owing to the use of photodiodes for positioning the crystal spectrometers, which interfere in the CCD of the RZP spectrometer.

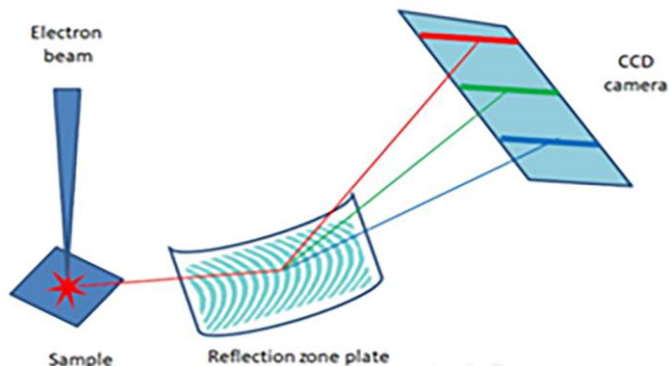


Fig. 1. Scheme of the dispersion and detection of the X-rays inside the reflection zone plate spectrometer. The zone plate is deposited on a spherical substrate. Adapted from from Nanooptics-Berlin: <https://www.nanooptics-berlin.com>.

3 Electronic structure

Most of the emissions falling in the ultra-soft X-ray range emission bands come from electron transitions taking place from the valence bands. Therefore, their energy distribution, *i.e.*, the shape of their spectrum, describes the occupied density of states in the valence band and so is sensitive to the chemical state of the emitting element. As an example, we show in figure 2(a) the Li-K α emission band from metallic lithium. The experimental spectrum is compared to the one simulated from the p occupied valence density of states calculated with the density functional theory. The DOS properly describes the shape and width of the band. The feature around 49 eV is related to the presence of either a small fraction of oxidised lithium in the sample or the existence of a plasmon satellite whose energy is expected about 7 eV [13] before the main peak.

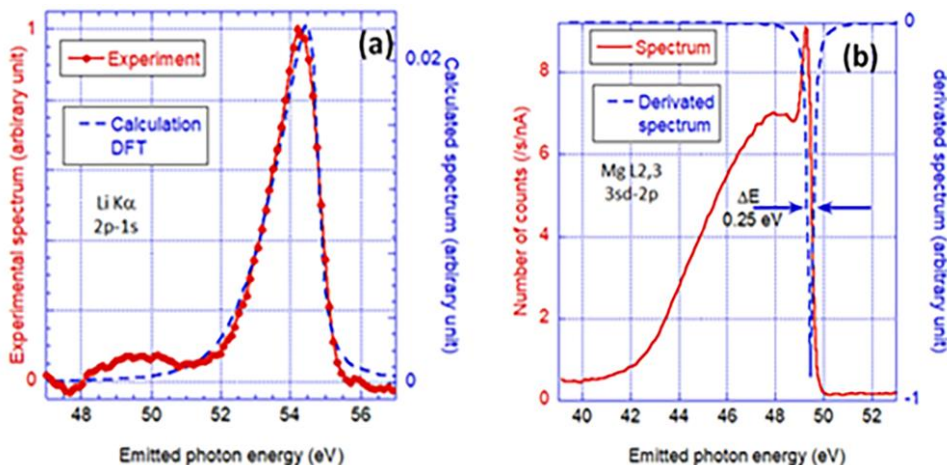


Fig. 2. a) Experimental and simulated Li-K emission bands of metallic lithium; b) Experimental Mg-L emission band of metallic magnesium and its derivative.

We show in figure 2(b) the Mg L_{2,3} experimental emission band of metallic magnesium. The sharp drop of intensity at 49 eV is another manifestation of the electronic structure. This drop marks the presence of the Fermi level, a sharp edge between the occupied and

unoccupied DOS. We take advantage of this edge to determine the spectral resolution of the spectrometer measured at the full width at half-maximum of the derivative spectrum, 0.25 eV in this case (another determination of resolution at the Fermi edge is the 25-75% measure). This value is then introduced in the simulations of the spectra to take the experimental broadening into account.

We now turn to the electronic structure of oxides and take silica (SiO_2) as an example. In this kind of compounds, the DOS is dominated by the ligand (oxygen in this case) DOS, see figure 3(a), the one of silicon (not shown) being about ten times less important. Another feature to emphasise is that the valence is separated in two parts by a forbidden gap: An upper valence band (UVB), close to the Fermi level coming mainly from the O p valence states and a lower valence band (LVB), located about 15 – 20 eV below the UVB, mainly due to the O s states. This description is also valid, for fluorides, nitrides, carbides and borides. However, the shift between the UVB and LVB depends on the electronegativity of the ligand: the larger the electronegativity, the greater the offset between the UVB and the LVB.

We show in figure 3(b) the Si $L_{2,3}$ emission spectrum of silicon obtained with electrons accelerated under 1 kV voltage, with a current of 140 nA and a dwell time of 100 s. With our apparatus, it is not possible to focus correctly the electron beam in this condition. Its size is estimated to be a few hundreds of nanometers. The low voltage enables observing the sample without charge effect and thus avoiding the deposition of a conductive coating. Because the emission band originates from electronic transition from the sd occupied states, it is superimposed to the Si s and Si d local and partial DOS calculated with the density functional theory as implemented in the Wien2k software [14]. The local DOS refers to the DOS calculated around an element in a multi-element compound. The partial DOS refers to a particular symmetry of the states. The comparison allows interpreting the observed spectrum: the main peak around 97 eV is due to the Si d states hybridised with the O p states; the one around 90 eV, to the Si s states mixed with the O p states; the one around 75 – 80 eV (the LVB) to the hybridisation of the Si sd states with the O s states. The energy difference of this last feature between the experimental and simulated spectra probably comes from the fact the sample is a sub-oxide, SiO_x , in the depth probed by the electrons.

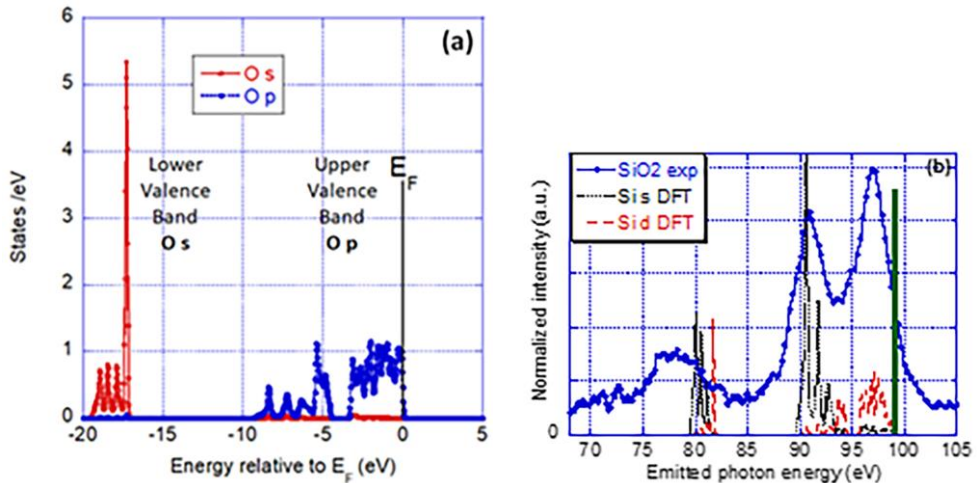


Fig. 3. (a) Local (oxygen) and partial (s and p) DOS of silica; (b) Experimental Si L emission band of silica compared to the local (silicon) and partial (s and d) DOS. The vertical bars mark the Fermi level.

It is important to rely on electronic structure calculations to correctly interpreting spectra of complicated materials. As an example, we show in figure 4 the spectrum of amblygonite, $(\text{Li},\text{Na})\text{AlPO}_4(\text{F},\text{OH})$, obtained under electron irradiation at 3 kV, a beam current of 100 nA,

a beam size of $5\ \mu\text{m}$ and a dwell time of 300 s. In addition to the interferences coming from the oxygen emission band diffracted at high orders, many features are present in the spectrum. Below 70 eV lies the Al $L_{2,3}$ emission band; the peaks between 60 and 65 eV are coming from the P $L_{2,3}$ emission band diffracted at the second order. This is confirmed when comparing with the simulated spectrum obtained from the P sd local and partial states calculation. In this range, there is also a contribution of the UVB of the Al L band. At first glance, the peak around 55 eV could be ascribed to the Li $K\alpha$ emission band owing to the expected photon energy of this emission. In fact, the simulation of the phosphorous spectrum shows that this peak arises from the LVB of the P L emission band, originating from the mixing of the P sd and O s valence states. In this case, the Li $K\alpha$ emission band cannot be observed owing to its very low intensity (low fluorescence yield and very small attenuation length of the order of 15 nm [15]) and to the strong interference with the P L emission band.

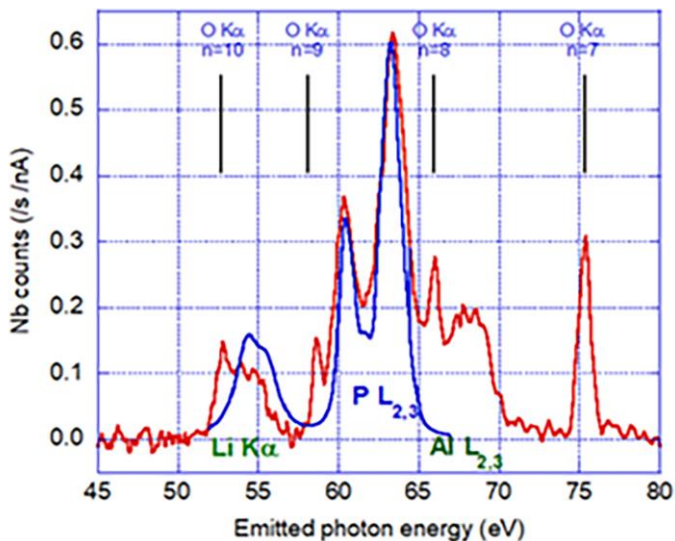


Fig. 4. Experimental spectrum of amblygonite (red line) compared to the second order diffracted P-L simulated spectrum (blue line).

4 Quantification attempt

We have tried to perform the elemental quantification of an AlCuLi quasi-crystal [16]. The Li $K\alpha$ and Al $L_{2,3}$ emission bands are shown in the spectrum presented in figure 5, obtained under 5 kV electron irradiation. Here the C K and O K interferences coming from the superficial contamination are well identified and their intensities can be subtracted from the intensities measured as the area under the peaks. The Li K and Al L intensities were compared to the ones of the pure metals to obtain the k -ratios, necessary as inputs in the quantification model. The AlCuLi quasi-crystal contains a significant amount of copper, and this will most likely modify the Al L and Li K spectral emissions [17]. We chose the PAP model [18] and mass absorption coefficient coming from the PENELoPE 2018 database [19]. As copper emission cannot be measured in this setup, its weight fraction was determined by difference. Following this process, the determined mass composition of the sample is the following: $\text{Al}_{0.57}\text{Cu}_{0.22}\text{Li}_{0.21}$. It is in good agreement with the $\text{Al}_{0.60}\text{Cu}_{0.17}\text{Li}_{0.23}$ composition determined by using the crystal spectrometers of the EPMA and working in the soft X-ray

range with the Al $K\alpha$ (1486 eV [20]) and Cu-L α (930 eV [20]) emissions. In this case, Li mass fraction was obtained by difference.

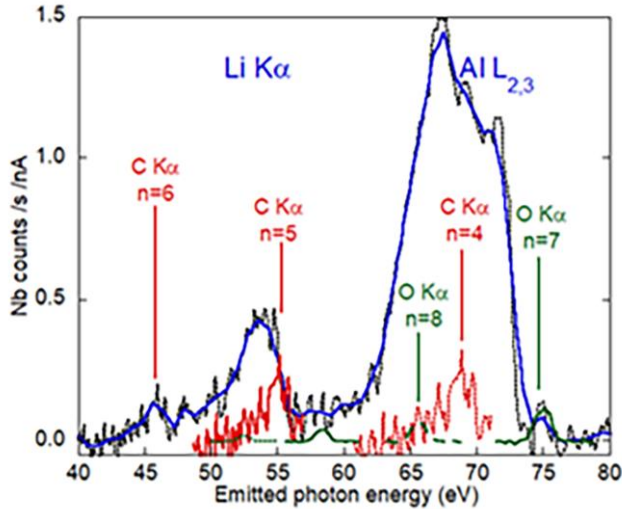


Fig. 5. Spectrum of an AlCuLi quasi-crystal measured in the 40 – 80 eV spectral range. The blue line is the smoothed spectrum.

We consider the quantification performed with the ultra-soft X-ray intensities only as an estimation as many factors with large uncertainties can affect the calculation of the mass fractions. Source of errors include: the background subtraction process; taking the intensities of the interfering C K and O K emissions into account; the oxidization of the surface of the AlCuLi sample together with the metallic Al and Li standards thus resulting in a multilayer problem; the presence of the weak Cu $M_{2,3}$ emission band in the studied spectral range; the attenuation of the radiation coming from the sample by the surface contamination; the possible presence of Al L satellite emissions in the Li K range; the suitability of the chosen quantification model; the lack of reliable mass attenuation coefficients in our spectral range; etc. Moreover, AlCuLi alloy is often multiphase when examined at high spatial resolution [21].

5 Conclusion

Grating spectrometers efficiently work on EPMA and SEM to study the ultra-soft X-ray range, *i.e.*, photon energies from a few tens of eV to some hundreds eV. They provide high resolution and since most emissions lying in this spectral range are emission bands, it is possible to study the electronic structure of solid materials. This kind of information is important to interpret the obtained spectra to ascribe the observed features to the correct elements. Additional work must be done on the sample environment (to minimise surface contamination) and data treatment (to improve intensity measurements) to be able to perform reliable elemental quantification.

This research was funded by Agence Nationale de la Recherche in the framework of the SQLX Project (ANR-20-CE29-0022). Participants to this project, K. Le Guen, K. Hassebi, N. Temmar, W. Aid, R. Benbalagh, R. Vacheresse, M.-C. Lépy, N. Rividi, M. Fialin, A. Verlaguet and G. Godard are thanked for their help.

A CC-BY public copyright license has been applied by the authors to the present document and will be applied to all subsequent versions arising from this submission, in accordance with the grant's open access conditions.

References

1. R. Van Grieken and A. Markowicz, editors, *Handbook of X-Ray Spectrometry*, 2nd ed. (CRC Press, Boca Raton, 2001).
2. K. Tsuji, J. Injuk, and R. Van Grieken, editors, *X-Ray Spectrometry: Recent Technological Advances* (John Wiley & Sons, 2005).
3. D. A. Wollman, S. W. Nam, D. E. Newbury, G. C. Hilton, K. D. Irwin, N. F. Bergren, S. Deiker, D. A. Rudman, and J. M. Martinis, *Nucl. Instrum. Methods Phys. Res. Sect. Accel. Spectrometers Detect. Assoc. Equip.* **444**, 145 (2000).
4. P. Hovington, V. Timoshevskii, S. Burgess, H. Demers, P. Statham, R. Gauvin, and K. Zaghbi, *Scanning* **38**, 571 (2016).
5. V. Polkonikov, N. Chkhalo, R. Pleshkov, A. Giglia, N. Rividi, E. Brackx, K. Le Guen, I. Ismail, and P. Jonnard, *Appl. Sci.* **11**, 6385 (2021).
6. K. Hassebi, E. Meltchakov, F. Delmotte, A. Giglia, and P. Jonnard, *Appl. Sci.* **14**, 956 (2024).
7. L. V. Azaroff, *X-Ray Spectroscopy*, McGraw-Hill Inc. (New York, 1974).
8. P. Schweizer, E. Brackx, and P. Jonnard, *Spectrochim. Acta Part B At. Spectrosc.* **218**, 106994 (2024).
9. M. Terauchi, *J. Electron Microsc. (Tokyo)* **50**, 101 (2001).
10. M. Terauchi and M. Kawana, *Microsc. Microanal.* **8**, 644 (2002).
11. A. Erko, A. Firsov, R. Gubzhokov, A. Bjeoumikhov, A. Günther, N. Langhoff, M. Bretschneider, Y. Höhn, and R. Wedell, *Opt. Express* **22**, 16897 (2014).
12. K. Hassebi, N. Rividi, M. Fialin, A. Verlaquet, G. Godard, J. Probst, H. Löchel, T. Krist, C. Braig, C. Seifert, R. Benbalagh, R. Vacheresse, V. Ilakovac, K. Le Guen, and P. Jonnard, *X-Ray Spectrom.* **54**, 76 (2025).
13. R. v. Baltz, in *Spectrosc. Dyn. Collect. Excit. Solids*, edited by B. Di Bartolo and S. Kyrkos (Springer US, Boston, MA, 1997), pp. 303–338.
14. P. Blaha, K. Schwarz, F. Tran, R. Laskowski, G. K. H. Madsen, and L. D. Marks, *J. Chem. Phys.* **152**, 074101 (2020).
15. CXRO X-ray interactions with matter, http://henke.lbl.gov/optical_constants/.
16. K. Hassebi, N. Rividi, O. Boudouma, M. Fialin, K. Le Guen, and P. Jonnard, *X-Ray Spectrom.* **54**, 171 (2025).
17. S. Rudinsky, C. M. MacRae, N. C. Wilson, H. Demers, and R. Gauvin, *Microsc. Microanal.* **25**, 250 (2019).
18. J.-L. Pouchou and F. Pichoir, *Rech. Aérospatiale* **5**, 349 (1984).
19. L. Sabbatucci and F. Salvat, *Radiat. Phys. Chem.* **121**, 122 (2016).
20. P. Jonnard and C. Bonnelle, *X-Ray Spectrom.* **40**, 12 (2011).
21. C. M. MacRae, A. E. Hughes, J. S. Laird, A. M. Glenn, N. C. Wilson, A. Torpy, M. A. Gibson, X. Zhou, N. Birbilis, and G. E. Thompson, *Microsc. Microanal.* **24**, 325 (2018).